Reduced noradrenergic innervation of ventral midbrain dopaminergic cell groups and the subthalamic nucleus in MPTP-treated parkinsonian monkeys

Gunasingh Jeyaraj Masilamoni[a,c], **Olivia Groover**[a,b], and **Yoland Smith**[a,b,c,*]

[a]Yerkes National Primate Research Center, Emory University, 954, Gatewood Rd NE, Atlanta, GA 30322, USA

[b]Department of Neurology, Emory University, 954, Gatewood Rd NE, Atlanta, GA 30322, USA

[c]Udall Center of Excellence for Parkinson's Disease, Emory University, 954, Gatewood Rd NE, Atlanta, GA 30322, USA

Abstract

There is anatomical and functional evidence that ventral midbrain dopaminergic (DA) cell groups and the sub-thalamic nucleus (STN) receive noradrenergic innervation in rodents, but much less is known about these interactions in primates. Degeneration of NE neurons in the locus coeruleus (LC) and related brainstem NE cell groups is a well-established pathological feature of Parkinson's disease (PD), but the development of such pathology in animal models of PD has been inconsistent across species and laboratories. We recently demonstrated 30–40% neuronal loss in the LC, A5 and A6 NE cell groups of rhesus monkeys rendered parkinsonian by chronic administration of 1-methyl-4-phenyl-1,2,3,6-tetrahydropyridine (MPTP). In this study, we used dopamine-beta-hydroxylase (DβH) immunocytochemistry to assess the impact of this neuronal loss on the number of NE terminal-like varicosities in the substantia nigra pars compacta (SNC), ventral tegmental area (VTA), retrorubral field (RRF) and STN of MPTP-treated parkinsonian monkeys. Our findings reveal that the NE innervation of the ventral mid-brain and STN of normal monkeys is heterogeneously distributed being far more extensive in the VTA, RRF and dorsal tier of the SNC than in the ventral SNC and STN. In parkinsonian monkeys, all regions underwent a significant (~50–70%) decrease in NE innervation. At the electron microscopic level, some DβH-positive terminals formed asymmetric axo-dendritic synapses in VTA and STN. These findings demonstrate that the VTA, RRF and SNCd are the main ventral midbrain targets of ascending NE inputs, and that these connections undergo a major break-down in chronically MPTP-treated parkinsonian monkeys. This severe degeneration of the ascending NE system may contribute to the pathophysiology of ventral midbrain and STN neurons in PD.

[*]Corresponding author at: Yerkes Primate Center, Emory University, 954, Gatewood Rd NE, Atlanta, GA 30329, USA. ysmit01@emory.edu (Y. Smith).

1. Introduction

Norepinephrine is an abundant and widely distributed neurotransmitter in the central nervous system (CNS). The LC contains more than half of brain NE neurons (Gaspar, 1994; Aston-Jones et al., 2000; Aston-Jones, 2004) and sends projections throughout the CNS (Lindvall et al., 1974; Swanson and Hartman, 1975; Jones et al., 1977; Jones and Moore, 1977; Carpenter et al., 1981; Foote et al., 1983; Nieuwenhuys et al., 1988; Geisler and Zahm, 2005). Although there is significant evidence for NE-mediated effects on various populations of midbrain dopamine (DA) neurons (Grenhoff and Svensson, 1988; Grenhoff et al., 1995), the ventral tegmental area (VTA) and the retrorubral field (RRF) receive a stronger NE innervation than the substantia nigra pars compacta (SNC) in rodents (Jones et al., 1977; Phillipson, 1979; Simon et al., 1979; Mejias-Aponte et al., 2009). Another basal ganglia target of NE afferents in rodents is the STN (Arcos et al., 2003; Belujon et al., 2007). Despite some advances in knowledge of the anatomy and physiology of NE in the rodent ventral midbrain and STN, much remains to be known about these interactions in primates (Ginsberg et al., 1993; Liprando et al., 2004; Vogt et al., 2008).

Degeneration of the LC and other brainstem NE cell groups is one of the pathological hallmarks of idiopathic PD and other neurodegenerative disorders (Chan-Palay and Asan, 1989; Chan-Palay, 1991). In fact, there is evidence that NE cell loss may occur prior to midbrain DA neurons degeneration in PD (Braak et al., 2003; Zarow et al., 2003; Halliday et al., 2006; Sotiriou et al., 2010). Animal models of PD have been inconsistent in mimicking NE cell loss (Forno et al., 1986; Gibb et al., 1989; Herrero et al., 1993), most likely due to differences in the type of toxins used, their regimen of administration, and the rigor with which quantitative methods were applied to assess these changes (Burns et al., 1983; Langston et al., 1984; Mitchell et al., 1985; Snyder and D'Amato, 1986; Gibb et al., 1989). Recently, we have reported 40% cell loss in LC and the adjoining A5 and A6 cell groups in rhesus monkeys chronically intoxicated with low doses of MPTP (Masilamoni et al., 2011), which is consistent with previous reports indicating that chronic low dose regimen of MPTP administration mimic much more closely the slow and progressive degeneration and dopaminergic and non-dopaminergic cell groups described in idiopathic PD (Forno et al., 1986; Hantraye et al., 1993; Fornai et al., 2005; Masilamoni et al., 2010).

In addition to its potential contribution to a wide range of non-motor deficits (autonomic dysfunction, psychiatric disorders, sleep disturbances, etc.…), the loss of NE neurons may contribute to the progressive degeneration of midbrain DA neurons in PD (Mavridis et al., 1991; Bing et al., 1994; Fornai et al., 1995; Srinivasan and Schmidt, 2003, 2004). Rodent studies have, indeed, suggested that NE may be neuroprotective towards midbrain DA neurons degeneration in mice models of PD (Mavridis et al., 1991; Fornai et al., 1997; Rommelfanger et al., 2004). Altogether, these data provide a solid foundation through which NE degeneration could play a critical role in the development of non-motor features and progressive loss of midbrain dopaminergic neurons in PD (Cash et al., 1987; Zweig et al., 1993; Bedard et al., 1998; Remy et al., 2005; Pintor et al., 2006; Marsh et al., 2009; Del Tredici and Braak, 2013).

Thus, to set the stage for a deeper understanding of NE functions in the ventral midbrain and STN of primates, the goals of the present study are two folds: (1) map the distribution, assess the relative abundance, and determine the synaptic connections of NE terminals in various DA cell groups and the STN of normal rhesus monkeys and (2) determine the extent of NE denervation these regions undergo in chronically MPTP-treated monkeys.

2. Material and methods

2.1. Animals

Six adult female rhesus monkeys (*Macaca mulatta*, 4.5–8.5 kg) from the Yerkes National Primate Research Center colony were used in this study, in accordance with guidelines from the National Institutes of Health. All procedures were approved by Emory's Animal Care and Use Committee. The animals were housed in a temperature-controlled room and exposed to a 12-h light/dark cycle. They were fed twice daily with monkey chow supplemented with fruits or vegetables. The animals had free access to water.

2.2. MPTP treatment and behavioral observations

The 6 rhesus monkeys used in this study were divided into two groups. Group 1 consisted of 3 animals that were treated with MPTP and Group 2 comprised 3 untreated monkeys that were used as control for DβH and tyrosine hydroxylase (TH) immunocytochemistry, and for varicosities and cell bodies counting. The MPTP regimen used to induce parkinsonism in these animals was reported elsewhere (Masilamoni et al., 2010). In brief, group 1 monkeys were trained to tolerate handling, transport and transfer in and out of behavioral cages. After habituation, baseline behavioral data were collected using a modified Parkinson's disease rating scale and other general locomotor activity rating methods routinely used in our laboratory (Masilamoni et al., 2010; Masilamoni et al., 2011).

Following collection of these baseline behavioral data, animals received weekly intramuscular injections of 0.2 mg/kg of MPTP (Sigma-Aldrich) for 17 weeks. The dosage of MPTP was then increased to 0.5 mg/kg for weeks 18 to 21. After the 21st MPTP injection, the monkeys displayed moderate parkinsonism (Motor Disability Score from 12 to 15.6 out of 27 points scale) (Masilamoni et al., 2011). At this point, the monkeys had received a cumulative MPTP dose of 33.8, 35.4, 39.8 mg. Because the parkinsonian rating scores did not significantly change 6 weeks after the last MPTP injection (11, 14 and 15, respectively), these monkeys were considered 'stably parkinsonian' (Masilamoni et al., 2010, 2011).

2.3. Termination of the experiment

At the end of the experiments, the monkeys were deeply anaesthetized with an overdose of pentobarbital (100 mg/kg, iv), and perfused transcardially with cold oxygenated Ringer's solution, followed by 2 l of fixative containing 4% paraformaldehyde and 0.1% glutaraldehyde in phosphate buffer (0.1 M, pH 7.4). After perfusion, the brains were removed from the skull and cut into 10 mm-thick blocks in the frontal plane. The blocks were further cut into 50 μm-thick sections with a vibratome and used for post-mortem immunostaining and cell counting procedures.

2.4. Immunohistochemistry

2.4.1. Pre-embedding immunoperoxidase for light microscopy—In order to validate the extent of NE innervation and its sensitivity to MPTP-induced degeneration in the ventral midbrain dopaminergic nuclei and the STN, brain sections from control and MPTP-treated monkeys were immunostained with specific antibodies against DβH (monoclonal rabbit anti-dopamine beta hydroxylase IgGs; Table 1). Some sections were immunostained for tyrosine hydroxylase (monoclonal mouse anti-tyrosine hydroxylase IgGs; Table 1) at a concentration of 1:1000 to identify DA neurons and define borders between the various midbrain cell groups. In addition, we used highly specific mouse monoclonal calbindin D28K antibodies at a concentration of 1:4000 (Sigma, catalogue number C9848; Table 1) to label calbindin-positive cells in the dorsal tier of the SNC (SNCd) and VTA, which allowed us to differentiate these neurons from the calbindin-negative ventral tier (SNCv) neurons (Masilamoni et al., 2010) (see Suppl. Fig. 1).

The immunostaining protocols used to localize the various antigens were described in our previous studies (Masilamoni et al., 2010, 2011). In brief, sections were treated at room temperature (RT) with sodium borohydride for 20 min followed by a pre-incubation for 1 h in a solution containing 1% normal horse serum or normal goat serum (NGS), 0.3% Triton-X-100, and 1% bovine serum albumin (BSA) in PBS. Sections were then incubated for 24 h at RT in a solution containing the subsequent primary antibodies in 1% normal horse or goat serum, 0.3% Tri-ton-X-100, and 1% BSA in PBS. Further details about the sources and antigen specificity of these antibodies are provided in Table 1. On the following day, sections were thoroughly rinsed in PBS and then incubated in a PBS solution containing either (secondary) biotinylated horse anti-goat IgGs, goat anti-rat IgGs, or goat anti-rabbit IgGs (1:200; Vector, Burlingame, CA) combined with 1% normal horse or goat serum, 0.3% Triton-X-100, and 1% BSA for 90 min at RT. Sections were exposed to an avidin-biotin-peroxidase complex (ABC; 1:100 [Vector] for 90 min followed by rinses in PBS and Tris buffer (50 mM; pH 7.6). Sections were then incubated within a solution containing 0.025% 3,3′-diamino-benzidine tetrahydrochloride (DAB; Sigma, St. Louis, MO), 10 mM imidazole, and 0.005% hydrogen peroxide in Tris buffer for 10 min at RT, rinsed with PBS, placed onto gelatin-coated slides, and cover slipped with Permount. Lastly, the sections were analyzed by using a Leica DMLB light microscope (Vienna, Austria) and scanned using a Scan Scope light microscope (Aperio Technologies, Vista, CA).

2.4.2. Pre-embedding immunoperoxidase for electron microscopy—To characterize the ultrastructural features of NE terminals in the ventral midbrain and STN, some sections were processed using the pre-embedding immunoperoxidase method to localize DβH at the electron microscopic level. In brief, series of STN and midbrain sections from 3 normal monkeys were transferred to a cryoprotectant solution containing 25% sucrose and 10% glycerol in PB (0.05 M, pH 7.4) for 20 min and then placed in a −80 °C freezer for 20 min to permeabilize cell membranes. They were then thawed through washes in decreasing concentrations of cryoprotectant solution until being washed in PBS. The subsequent tissue processing was identical to that used for light microscopy, up to the point of DAB exposure, with two important differences: Triton X-100 was omitted from all solutions, and sections were incubated in the primary antibody solution for 48 h at 4 °C.

After DAB exposure, the tissue was rinsed in PB (0.1 M, pH 7.4) and treated with 1% osmium tetroxide for 20 min. It was then rinsed with PB and dehydrated with increasing concentrations of ethanol, up to 100%. Uranyl acetate (1%) was added to the 70% EtOH dehydration solution and incubated for 35 min in order to increase the contrast of membranes in the electron microscope. After alcohol dehydration, sections were treated with propylene oxide, embedded in epoxy resin (Durcupan ACM; Fluka, Buchs, Switzerland) for at least 12 h, mounted onto slides, and placed in a 60 °C oven for 48 h to cure the resin.

2.4.2.1. Electron microscopic observations: To confirm that DβH-positive varicosities seen at the light microscopic level were vesicle-containing axon terminals, two blocks of tissue from the VTA and STN of one control monkey that displayed optimal ultrastructural preservation and DβH staining were cut out from the embedded sections and glued onto resin blocks for ultrathin sectioning with an ultramicrotome (Leica Ultracut T2). Sixty-nanometer-thick sections were collected from the surface of the tissue block to ensure that antibody penetration was optimal. Sections were mounted on single-slot pioloform-coated copper grids, stained for 5 min with lead citrate, and examined with a JEOL transmission electron microscope (EM; model 1011, Jeol, Peabody, MA). Electron micrographs were captured and saved with a CCD camera (Model 785; Warrendale, PA) controlled by Digital Micrograph software (version 3.11.1; Gatan, Inc.). Immunoperoxidase labeling for DβH could be identified as a dark, amorphous deposit in the neuronal elements. Immunoreactive elements were classified based on ultrastructural features (Peters et al., 1991). A total of fifty micrographs of randomly-encountered DAB-labeled axon terminals were captured at 50,000× in the VTA and STN.

2.5. Estimation of the number of DβH-positive varicosities

Unbiased sampling of labeled varicosities in the ventral midbrain and STN was applied to determine regional differences in the density of DβH-containing varicosities across various regions of the ventral midbrain and STN in normal and MPTP-treated monkeys. The unbiased estimation of the total number of DβH-positive varicosities in SNCv, SNCd, VTA, RRF and STN was determined using the optical fractionator principle (StereoInvestigator, MicroBrightField, Inc., Williston, VT). For this analysis, DβH-positive varicosities were defined as individual round or oval-shaped bulbous structures spaced irregularly along labeled axons that varied in size from 0.5 to 3.0 μm in diameter. In some cases, clusters of varicosities were attached at the end of short stalks which originated from a parent labeled axon (Fig. 2E and G). The random systematic sampling of counting areas was done using the Leica DMR microscope. First, we took low power micrographs (1.25×) of TH- and CB-immunostained ventral midbrain sections, and manually delineated the borders of SNCv vs SNCd, and VTA, based on the absence or presence of CB immunoreactivity, respectively (Suppl. Fig. 1). Then, the borders of the different ventral midbrain regions were manually delineated on DβH- and TH-immunolabeled slides adjacent to those immunostained for CB. Counts of DβH-immunoreactive varicosities and TH-positive neurons were generated using a 100× oil immersion objective. To perform unbiased stereology, counting frames (65 × 65 μm) were randomly placed by the stereology software within the chosen region of interest. The software also controlled the position of the x–y stage of the microscope, so that the entire nuclei could be scanned by successively meandering between counting frames. The

software calculated the estimated total number of DβH-positive varicosities in the different subnuclei. Measurements were made from 1 of 12 serial sections through the rostrocaudal extent of these nuclei. The number of labeled varicosities was counted in a total of 4, 12, 11, 10 and 4 sections of the STN, SNCv, SNCd, VTA and RRF, respectively. This design resulted in a coefficient of error of 0.027–0.067 (Gundersen, m = 1) (Gundersen and Osterby, 1981). The density of labeled varicosities was calculated by dividing the total number of varicosities counted in each nucleus by the estimated volume of the nuclei.

We used the Cavalieri's principle to estimate the volume of the SNCv, SNCd, VTA, RRF and STN from TH-immunostained sections in three controls and three parkinsonian monkeys (Gundersen and Osterby, 1981; Schmitz and Hof, 2005). The boundary of each nuclei was delineated by TH- and CB-immunostained elements as explained above. Measurements were made from 1 of 12 serial sections through the rostrocaudal extent of these nuclei.

3. Results

3.1. Motor impairment and nigrostriatal dopamine loss in MPTP-treated parkinsonian monkeys

Chronic low dose MPTP exposure was used in this study to slowly induce progressive parkinsonian motor signs and nigrostriatal dopaminergic denervation in three monkeys. A detailed description of this MPTP treatment protocol, and quantitative data about parkinsonian motor scores, extent of striatal dopamine denervation and nigral dopaminergic neurons loss are provided in our previous studies, and will not be repeated here (Masilamoni et al., 2010; Masilamoni et al., 2011). In brief, after the last injection of MPTP, the monkeys displayed stable moderate parkinsonian symptoms, including akinesia, bradykinesia, rigidity, postural instability, mask-like faces for at least 6 weeks prior to sacrifice. In postmortem tissue, TH immunostaining was significantly decreased in the whole striatum, but most particularly in the post-commissural and anterolateral putamen than in the caudate nucleus, anteromedial putamen and nucleus accumbens (Fig. 1A–D). As expected, this striatal denervation was accompanied with a significant loss of TH-immunoreactive neurons in the SNCv, but not as pronounced in the SNCd and VTA (Fig. 1E, F). There were highly significant differences ($P < 0.001$) in the extent of cell loss in the different ventral midbrain dopaminergic cell groups. The loss was more severe in the SNCv (71%) than in the SNCd (59%) and in VTA (48%). As previously described (Masilamoni et al., 2010), these animals displayed a 30–40% loss of noradrenergic neurons in the LC and related A5 and A7 noradrenaline cell groups (Fig. 1G, H).

3.2. Morphological characteristics and ultrastructural features of DβH-positive varicosities in the ventral midbrain and STN

At the light microscopic level, DβH-positive varicose fibers were found through the full extent of the ventral midbrain dopaminergic cells groups, but were particularly abundant in the VTA, RRF and SNCd. Only scarce elements were found in the SNCv (Fig. 2A–F). In general, beaded axonal-like profiles and terminal-varicosities which were either isolated within the neuropil or part of pericellular baskets around the cell bodies or proximal

dendrites (Fig. 2A–F). The pericellular innervation was most prevalent in the VTA and RRF, though it could occasionally be seen in the SNCd, but not in the SNCv. In the STN, DβH immunoreactivity was faint and associated predominantly with thin long varicose axon-like processes that were sparsely distributed throughout the nucleus (Fig. 2G).

To confirm that the DβH-positive varicose processes seen at the light microscopic level correspond to axon terminals, an electron microscopic analysis was performed on two blocks of tissue from the VTA and the STN of a control monkey. At the ultrastructural level, DβH immunoreactivity was expressed either in small unmyelinated axons or in the pre-synaptic active zones of axon terminals in both the STN and VTA (Fig. 3A–D). The labeled boutons displayed ultrastructural features reminiscent of those previously described for terminals immunoreactive for norepinephrine transporter in the rodent VTA (Liprando et al., 2004) i.e. they were small to medium-sized (~0.3–1.2 μm in diameter), contained a few mitochondria as well as a variable number of small round and pleomorphic synaptic vesicles. In cases that the synaptic specialization could be seen in the plane of single ultrathin section, it was of the asymmetric type (Fig. 3A–D).

3.3. The RRF and VTA receive the densest noradrenergic innervation in the ventral midbrain of normal rhesus monkeys

The density of DβH-positive axons and varicosities varied significantly across different DA regions of the ventral midbrain and the STN; the strongest DβH-positive innervation being found in RRF and VTA (Figs. 2C, D: 5). Albeit to a lower degree, the SNCd also received a moderate NE innervation, while the SNCv and STN contained only scarce DβH-positive profiles in normal monkeys (Fig. 2F, G). Counts of DβH-positive varicosities confirmed these observations showing that the RRF was the most densely innervated region (656.1×10^4 varicosities/mm^3) followed by the VTA (356.2×10^4 varicosities/mm^3), SNCd (178.4×10^4 varicosities/mm^3), SNCv (67.5×10^4 varicosities/mm^3) and STN (7.5×10^4 varicosities/mm^3) (Fig. 4C). Our quantitative analysis further highlighted specific patterns of distribution of DβH-positive varicosities along the rostrocaudal axis of the different nuclei examined such that the density of DβH-labeled varicose processes was greatest in the rostral tier of the RRF, while it reached its peak in the middle tier of VTA (Figs. 4A, B; 5). The caudal and rostral tiers of the SNCv and SNCd were the most massively innervated regions of these sub-nuclei, respectively (data not shown).

3.4. Reduced noradrenergic innervation of dopaminergic cell groups and STN in MPTP-treated monkeys

To assess changes in the abundance of DβH-positive terminals in parkinsonian animals, we compared the distribution of DβH–immunopositive varicosities between normal and MPTP-treated monkeys. Our light microscopic observations showed that chronic low dose MPTP treatment significantly decreased the density of NE innervation in the ventral midbrain and STN of parkinsonian monkeys compared to control. Our stereological quantitative assessment of the number of labeled varicosities showed that the STN contained 542,663 DβH-immunopositive varicosities, while this density was 66% lower (183,642) in parkinsonian animals (Fig. 4C). The difference between normal and parkinsonian monkeys was significant ($P < 0.001$). The decrease in DβH-immunopositive varicosities appeared to

be roughly similar across the midbrain DA groups in the SNCv (46% loss), SNCd (69% loss) VTA (74% loss) and RRF (59% loss) in the parkinsonian monkeys (Fig. 4C).

4. Discussion

The results of this study reveal new aspects of the distribution and structural features of NE terminals in the ventral midbrain and STN of nonhuman primates. Our findings demonstrate that the RRF, VTA and SNCd are areas most enriched in NE terminals, while the SNCv and STN receive a much sparser noradrenergic innervation in primates. At the ultrastructural level, NE terminals in the monkey VTA and STN display similar ultrastructural features, occasionally form asymmetric axodendritic synapses, and structurally resemble NE terminals in the rodent VTA. In line with our previous findings of significant NE cell loss in the LC of chronically MPTP-treated monkeys, our quantitative analysis demonstrates a 40–50% loss of DβH-positive terminal-like varicosities in all ventral midbrain regions and the STN of parkinsonian monkeys. Taken together with our previous data, these results provide strong evidence that monkeys treated chronically with low doses of MPTP undergo severe NE neuronal loss and a major breakdown of the noradrenergic innervation of midbrain dopaminergic cell groups and STN. Knowing the critical regulatory, and possibly neuroprotective, role of NE afferents towards degeneration of midbrain dopaminergic neurons in parkinsonism, our findings set the stage for future studies aimed at better understand the physiological and pathological consequences of degeneration of the ascending NE system in Parkinson's disease.

4.1. Noradrenergic afferents to midbrain DA neuron and its functional implications in PD

Results of our light microscopic observations and stereological analyses from normal monkeys are consistent with those previously described in rodents, showing that the RRF and VTA receive the densest NE innervation among the ventral midbrain DA cell groups (Aston-Jones, 2004; Mejias-Aponte et al., 2009). These anatomical findings corroborate electrophysiological and pharmacological evidence that ascending noradrenergic afferents regulate the activity of midbrain dopaminergic neurons and/or release of dopamine in the striatum and cerebral cortex (Snoddy and Tessel, 1985; Gonon, 1988; Bean and Roth, 1991; Delaville et al., 2012).

NE acts via two G-protein receptor families, α (α1, α2), and β (subtype β1, β2, β3), each consisting of several subtypes (Wikberg, 1982). In the CNS, α_1 and β receptors are primarily expressed at postsynaptic sites, where they generally mediate an excitatory action, while α_2 receptors are often located pre-synaptically, and exert inhibitory effects on transmitter release (Kawasaki et al., 2003; Otmakhova et al., 2005; Ferry et al., 2015). The electrical stimulation of LC and pharmacological blockade of α_2 adrenergic receptors influence the activity of midbrain DA neurons (Grenhoff and Svensson, 1993) by decreasing potassium conductance, inhibiting metabotropic glutamate receptor (mGluR)-mediated IPSPs, or through a non-selective cationic conductance (Grenhoff et al., 1995; Paladini et al., 2001; Cathala et al., 2002). On the other hand, α_1 adrenoceptors antagonist reduces burst firing in these cells (Grenhoff and Svensson, 1988, 1993; Grenhoff et al., 1995) through an

activation of a calcium dependent potassium conductance and an increase in GABA release (Paladini et al., 2001; Cathala et al., 2002; Dumont and Williams, 2004).

In light of these findings, our data showing a major loss of NE terminals in the ventral midbrain of MPTP-treated parkinsonian monkeys strongly suggest that such denervation could impact significantly upon the firing rate and pattern of activity of mesocortical and nigrostriatal dopaminergic neurons in primates. Future studies are needed to further characterize the regulatory functions of NE on mid-brain dopaminergic cell groups' activity in normal and parkinsonian monkeys.

4.2. Sources of ascending NE afferents to ventral midbrain dopaminergic cell groups

Although the exact sources of NE inputs to the ventral midbrain remain poorly characterized in primates, this issue has been examined in more detail in rats (Jones et al., 1977; Phillipson, 1979; Geisler and Zahm, 2005; Mejias-Aponte et al., 2009) by means of retrograde and anterograde tracing methods. In brief, these studies revealed that neuronal populations in various brainstem noradrenergic cell groups (A1, A2, A5 and LC) send projections to the VTA and RRF, while inputs to the SN are far less prominent and largely arise from the LC. Axonal projections from these various cell groups likely account for the majority of DβH-immunoreactive terminals described in the present study.

However, some of these DβH-positive terminals may also originate from brainstem adrenergic cell groups (C1,C2,C3), but these probably comprise only a small proportion of labeled terminals in the VTA and SN (Mejias-Aponte et al., 2009), although the RRF may receive a stronger adrenergic innervation than other cell groups (Mejias-Aponte et al., 2009). These adrenergic and noradrenergic cell groups receive inputs from a wide variety of lower brainstem centers that carry information related to homeostatic regulation, suggesting their involvement in regulating the physiological well-being of organisms (Aston-Jones and Bloom, 1981; Blessing and Willoughby, 1985; Rinaman, 2003; Hilaire et al., 2004; Guyenet, 2006). Another important function of these ascending systems might be to regulate increased burst firing in midbrain dopaminergic neurons during stress, a physiological effect that is modulated by alpha-1 and alpha-2 adrenoreceptors (Grenhoff and Svensson, 1988, 1993; Paladini et al., 2001). The possible role of ascending LC inputs in regulating cognitive performance through interactions with midbrain dopaminergic neurons has also been suggested (Aston-Jones and Cohen, 2005).

Thus altogether, these data indicate that the degeneration of noradrenergic inputs to the ventral midbrain in PD may contribute to a wide variety of motor a non-motor symptoms of the disease. Further studies of the functional effects of noradrenergic systems degeneration in MPTP-treated monkeys would help translate these observations to the human diseased condition.

4.3. Neuroprotective effects of NE on SNc dopaminergic neurons degeneration?

Beyond its role as a classic neurotransmitter, some evidence suggests that NE may exert neuroprotective influence upon midbrain dopaminergic neurons in MPTP- or 6-OHDA-treated nonhuman primate and rodent models of parkinsonism (Mavridis et al., 1991; Marien et al., 1993; Bing et al., 1994; Fornai et al., 1997). In these studies, lesion of noradrenergic

neurons potentiated the toxin-induced damage of nigrostriatal dopaminergic cells. In line with these data, blockade of the norepinephrine transporter was found to protect midbrain dopaminergic neurons from MPTP-induced degeneration in mice (Rommelfanger et al., 2004). Although the mechanisms that underlie these neuroprotective effects remain to be established, in vitro studies have described NE as a mediator of anti-inflammatory actions (Galea et al., 2003), antioxidant effects (Troadec et al., 2001; Mourlevat et al., 2003; Traver et al., 2005), and inhibitor of nitric oxide synthase production (Feinstein et al., 1993; Dello Russo et al., 2004). The combination of these properties likely contributes to the neuroprotective effects of NE.

It is noteworthy that the pattern of midbrain dopaminergic neuronal loss in Parkinson's disease follows a pattern of degeneration that is inversely correlated with the extent of NE innervation of the ventral mid-brain i.e. DA loss is more extensive in SNCv, which receives sparse NE inputs, than in the SNCd, VTA and RRF (Fearnley and Lees, 1991), which contain a far greater number of NE terminals. Thus, it is tempting to speculate that the strong NE innervation of VTA and RRF regions may be responsible for the selective sparing of a large proportion of dopaminergic neurons in these regions in the parkinsonian condition. The neuroprotective role of NE has also been suggested in mouse models of Alzheimer's disease (Jardanhazi-Kurutz et al., 2010).

4.4. Noradrenergic innervation of the STN

Our light and electron microscopic data provide evidence for a sparse to moderate noradrenergic innervation of the STN in rhesus monkey. At the ultrastructural level, DβH-positive terminals in the monkey STN display similar features to those seen in the monkey and rodent VTA (Liprando et al., 2004). These data are consistent with results of tract tracing studies showing a small number of retrogradely labeled neurons in the LC after STN injections (Carpenter et al., 1981; Canteras et al., 1990; Parent and Hazrati, 1995) and previous histochemical studies of DβH fibers in the monkey and rodent STN (Swanson and Hartman, 1975; Ginsberg et al., 1993). Despite this modest innervation, patch clamp recording studies have shown that modulation of pre-synaptic alpha-2 or post-synaptic alpha-1 adrenergic receptors have a significant effect on the firing of STN neurons in rat brain slices (Arcos et al., 2003; Belujon et al., 2007). In light of these findings, it has been suggested that direct NE innervation of the STN may play a role in mediating some of the antiparkinsonian effects of alpha-2 noradrenergic receptor antagonists in animal models of PD (Mavridis et al., 1991; Bezard et al., 1999; Chopin et al., 1999; Belujon et al., 2007; Coenen et al., 2008).

Thus, despite its modest nature, the NE innervation of the STN has some functional relevance, suggesting that the partial loss of NE innervation of the STN described in our study could potentially contribute to the abnormal firing rate and bursting pattern of STN neurons in parkinsonism. Knowing the importance of abnormal STN outflow in the parkinsonian state, a deeper understanding of the mechanisms by which NE regulates STN neuronal activity in primates is warranted.

4.5. Concluding remarks

Despite well-established evidence that brainstem NE neurons in the locus coeruleus and related brainstem cell groups degenerate in PD (Greenfield and Bosanquet, 1953; Ehringer and Hornykiewicz, 1960, 1998), sometimes to a greater extent than in SNc (Zarow et al., 2003), the importance of this degeneration in the development of motor and non-motor symptoms of the disease remains poorly understood. Because the majority of PD-related studies make use of animal models that display limited or no significant loss of NE cell groups, much remains to be known about the exact involvement of NE neuronal loss in PD pathophysiology. Results from this study and previous data from our laboratory and others (Mitchell et al., 1985; Di Paolo et al., 1986; Forno et al., 1986; Masilamoni et al., 2011; Delaville et al., 2012; Pifl et al., 1991) demonstrate that chronic MPTP administration in nonhuman primates results in significant NE cell loss, and prominent denervation of key brain regions that could contribute to a wide range of motor, psychiatric, cognitive and autonomic dysfunctions commonly seen in PD patients (Olanow et al., 2011). The use of such an animal model in future behavioral and physiological studies should help better understand the role of NE denervation in PD pathophysiology, and assess more thoroughly the potential therapeutic benefits of NE-related drugs in this disorder (Delaville et al., 2012).

Supplementary data to this article can be found online at http://dx.doi.org/10.1016/j.nbd. 2016.12.025.

Acknowledgments

References

Arcos D, Sierra A, Nunez A, Flores G, Aceves J, Arias-Montano JA. Noradrenaline increases the firing rate of a subpopulation of rat subthalamic neurones through the activation of alpha 1-adrenoceptors. Neuropharmacology. 2003; 45:1070–1079. [PubMed: 14614950]

Aston-Jones, G. Locus coeruleus, A5 and A7 noradrenergic cell groups. In: Paxinos, G., editor. The Rat Nervous System. Elsevier Academic Press; Amsterdam: 2004. p. 259-294.

Aston-Jones G, Bloom FE. Norepinephrine-containing locus coeruleus neurons in behaving rats exhibit pronounced responses to non-noxious environmental stimuli. J Neurosci. 1981; 1:887–900. [PubMed: 7346593]

Aston-Jones G, Cohen JD. Adaptive gain and the role of the locus coeruleus-norepinephrine system in optimal performance. J Comp Neurol. 2005; 493:99–110. [PubMed: 16254995]

Aston-Jones G, Rajkowski J, Cohen J. Locus coeruleus and regulation of behavioral flexibility and attention. Prog Brain Res. 2000; 126:165–182. [PubMed: 11105646]

Bean AJ, Roth RH. Effects of haloperidol administration on in vivo extracellular dopamine in striatum and prefrontal cortex after partial dopamine lesions. Brain Res. 1991; 549:155–158. [PubMed: 1909923]

Bedard MA, el Massioui F, Malapani C, Dubois B, Pillon B, Renault B, Agid Y. Attentional deficits in Parkinson's disease: partial reversibility with naphtoxazine (SDZ NVI-085), a selective noradrenergic alpha 1 agonist. Clin Neuropharmacol. 1998; 21:108–117. [PubMed: 9579297]

Belujon P, Bezard E, Taupignon A, Bioulac B, Benazzouz A. Noradrenergic modulation of subthalamic nucleus activity: behavioral and electrophysiological evidence in intact and 6-hydroxydopamine-lesioned rats. J Neurosci. 2007; 27:9595–9606. [PubMed: 17804620]

Bezard E, Brefel C, Tison F, Peyro-Saint-Paul H, Ladure P, Rascol O, Gross CE. Effect of the alpha 2 adrenoreceptor antagonist, idazoxan, on motor disabilities in MPTP-treated monkey. Prog Neuro-Psychopharmacol Biol Psychiatry. 1999; 23:1237–1246.

Bing G, Zhang Y, Watanabe Y, McEwen BS, Stone EA. Locus coeruleus lesions potentiate neurotoxic effects of MPTP in dopaminergic neurons of the substantia nigra. Brain Res. 1994; 668:261–265. [PubMed: 7704612]

Blessing WW, Willoughby JO. Excitation of neuronal function in rabbit caudal ventrolateral medulla elevates plasma vasopressin. Neurosci Lett. 1985; 58:189–194. [PubMed: 2864668]

Braak H, Del Tredici K, Rub U, de Vos RA, Jansen Steur EN, Braak E. Staging of brain pathology related to sporadic Parkinson's disease. Neurobiol Aging. 2003; 24:197–211. [PubMed: 12498954]

Burns RS, Chiueh CC, Markey SP, Ebert MH, Jacobowitz DM, Kopin IJ. A primate model of parkinsonism: selective destruction of dopaminergic neurons in the pars compacta of the substantia nigra by N-methyl-4-phenyl-1,2,3,6-tetrahydropyridine. Proc Natl Acad Sci U S A. 1983; 80:4546–4550. [PubMed: 6192438]

Canteras NS, Shammah-Lagnado SJ, Silva BA, Ricardo JA. Afferent connections of the subthalamic nucleus: a combined retrograde and anterograde horseradish peroxidase study in the rat. Brain Res. 1990; 513:43–59. [PubMed: 2350684]

Carpenter MB, Carleton SC, Keller JT, Conte P. Connections of the subthalamic nucleus in the monkey. Brain Res. 1981; 224:1–29. [PubMed: 7284825]

Cash R, Dennis T, L'Heureux R, Raisman R, Javoy-Agid F, Scatton B. Parkinson's disease and dementia: norepinephrine and dopamine in locus ceruleus. Neurology. 1987; 37:42–46. [PubMed: 3796837]

Cathala L, Guyon A, Eugene D, Paupardin-Tritsch D. Alpha2-adrenoceptor activation increases a cationic conductance and spontaneous GABAergic synaptic activity in dopaminergic neurones of the rat substantia nigra. Neuroscience. 2002; 115:1059–1065. [PubMed: 12453479]

Chan-Palay V. Alterations in the locus coeruleus in dementias of Alzheimer's and Parkinson's disease. Prog Brain Res. 1991; 88:625–630. [PubMed: 1726030]

Chan-Palay V, Asan E. Quantitation of catecholamine neurons in the locus coeruleus in human brains of normal young and older adults and in depression. J Comp Neurol. 1989; 287:357–372. [PubMed: 2570793]

Chopin P, Colpaert FC, Marien M. Effects of alpha-2 adrenoceptor agonists and antagonists on circling behavior in rats with unilateral 6-hydroxydopamine lesions of the nigrostriatal pathway. J Pharmacol Exp Ther. 1999; 288:798–804. [PubMed: 9918591]

Coenen VA, Gielen FL, Castro-Prado F, Abdel Rahman A, Honey CR. Noradrenergic modulation of subthalamic nucleus activity in human: metoprolol reduces spiking activity in microelectrode recordings during deep brain stimulation surgery for Parkinson's disease. Acta Neurochir. 2008; 150:757–762. (discussion 762). [PubMed: 18574545]

Del Tredici K, Braak H. Dysfunction of the locus coeruleus-norepinephrine system and related circuitry in Parkinson's disease-related dementia. J Neurol Neurosurg Psychiatry. 2013; 84:774–783. [PubMed: 23064099]

Delaville C, Chetrit J, Abdallah K, Morin S, Cardoit L, De Deurwaerdere P, Benazzouz A. Emerging dysfunctions consequent to combined monoaminergic depletions in Parkinsonism. Neurobiol Dis. 2012; 45:763–773. [PubMed: 22079236]

Dello Russo C, Boullerne AI, Gavrilyuk V, Feinstein DL. Inhibition of microglial inflammatory responses by norepinephrine: effects on nitric oxide and interleukin-1beta production. J Neuroinflammation. 2004; 1:9. [PubMed: 15285793]

Di Paolo T, Bedard P, Daigle M, Boucher R. Long-term effects of MPTP on central and peripheral catecholamine and indoleamine concentrations in monkeys. Brain Res. 1986; 379:286–293. [PubMed: 2427166]

Dumont EC, Williams JT. Noradrenaline triggers GABAA inhibition of bed nucleus of the stria terminalis neurons projecting to the ventral tegmental area. J Neurosci. 2004; 24:8198–8204. [PubMed: 15385602]

Ehringer H, Hornykiewicz O. Distribution of noradrenaline and dopamine (3-hydroxytyramine) in the human brain and their behavior in diseases of the extrapyramidal system. Klin Wochenschr. 1960; 38:1236–1239. [PubMed: 13726012]

Ehringer H, Hornykiewicz O. Distribution of noradrenaline and dopamine (3-hydroxytyramine) in the human brain and their behavior in diseases of the extrapyramidal system. Parkinsonism Relat Disord. 1998; 4:53–57. [PubMed: 18591088]

Fearnley JM, Lees AJ. Ageing and Parkinson's disease: substantia nigra regional selectivity. Brain. 1991; 114(Pt 5):2283–2301. [PubMed: 1933245]

Feinstein R, Kanety H, Papa MZ, Lunenfeld B, Karasik A. Tumor necrosis factor-alpha suppresses insulin-induced tyrosine phosphorylation of insulin receptor and its substrates. J Biol Chem. 1993; 268:26055–26058. [PubMed: 8253716]

Ferry B, Parrot S, Marien M, Lazarus C, Cassel JC, McGaugh JL. Noradrenergic influences in the basolateral amygdala on inhibitory avoidance memory are mediated by an action on alpha2-adrenoceptors. Psychoneuroendocrinology. 2015; 51:68–79. [PubMed: 25286225]

Foote SL, Bloom FE, Aston-Jones G. Nucleus locus ceruleus: new evidence of anatomical and physiological specificity. Physiol Rev. 1983; 63:844–914. [PubMed: 6308694]

Fornai F, Bassi L, Torracca MT, Scalori V, Corsini GU. Norepinephrine loss exacerbates methamphetamine-induced striatal dopamine depletion in mice. Eur J Pharmacol. 1995; 283:99–102. [PubMed: 7498327]

Fornai F, Bassi L, Bonaccorsi I, Giorgi F, Corsini GU. Noradrenaline loss selectivity exacerbates nigrostriatal toxicity in different species of rodents. Funct Neurol. 1997; 12:193–198. [PubMed: 9218976]

Fornai F, Schluter OM, Lenzi P, Gesi M, RNucleus locus ceruleusuffoli R. Ferrucci M, Lazzeri G, Busceti CL, Pontarelli F, Battaglia G, Pellegrini A, Nicoletti F, Ruggieri S, Paparelli A, Sudhof TC. Parkinson-like syndrome induced by continuous MPTP infusion: convergent roles of the ubiquitin-proteasome system and alpha-synuclein. Proc Natl Acad Sci U S A. 2005; 102:3413–3418. [PubMed: 15716361]

Forno LS, Langston JW, DeLanney LE, Irwin I, Ricaurte GA. Locus ceruleus lesions and eosinophilic inclusions in MPTP-treated monkeys. Ann Neurol. 1986; 20:449–455. [PubMed: 3024555]

Galea E, Heneka MT, Dello Russo C, Feinstein DL. Intrinsic regulation of brain inflammatory responses. Cell Mol Neurobiol. 2003; 23:625–635. [PubMed: 14514020]

Gaspar, P. Anatomy of the Noradrenergic Pathways in the Primate Brain Alteration in Parkinson's Disease. CRC Press; Boca Raton: 1994. p. 73-88.

Geisler S, Zahm DS. Afferents of the ventral tegmental area in the rat-anatomical substratum for integrative functions. J Comp Neurol. 2005; 490:270–294. [PubMed: 16082674]

Gibb WR, Terruli M, Lees AJ, Jenner P, Marsden CD. The evolution and distribution of morphological changes in the nervous system of the common marmoset following the acute administration of 1-methyl-4-phenyl-1,2,3,6-tetrahydropyridine. Mov Disord. 1989; 4:53–74. [PubMed: 2494438]

Ginsberg SD, Hof PR, Young WG, Morrison JH. Noradrenergic innervation of the hypothalamus of rhesus monkeys: distribution of dopamine-beta-hydroxylase immunoreactive fibers and quantitative analysis of varicosities in the paraventricular nucleus. J Comp Neurol. 1993; 327:597–611. [PubMed: 8440783]

Gonon FG. Nonlinear relationship between impulse flow and dopamine released by rat midbrain dopaminergic neurons as studied by in vivo electrochemistry. Neuroscience. 1988; 24:19–28. [PubMed: 3368048]

Greenfield JG, Bosanquet FD. The brain-stem lesions in Parkinsonism. J Neurol Neurosurg Psychiatry. 1953; 16:213–226. [PubMed: 13109537]

Grenhoff J, Svensson TH. Clonidine regularizes substantia nigra dopamine cell firing. Life Sci. 1988; 42:2003–2009. [PubMed: 3367694]

Grenhoff J, Svensson TH. Prazosin modulates the firing pattern of dopamine neurons in rat ventral tegmental area. Eur J Pharmacol. 1993; 233:79–84. [PubMed: 8097162]

Grenhoff J, North RA, Johnson SW. Alpha 1-adrenergic effects on dopamine neurons recorded intracellularly in the rat midbrain slice. Eur J Neurosci. 1995; 7:1707–1713. [PubMed: 7582125]

Gundersen HJ, Osterby R. Optimizing sampling efficiency of stereological studies in biology: or 'do more less well!'. J Microsc. 1981; 121:65–73. [PubMed: 7014910]

Guyenet PG. The sympathetic control of blood pressure. Nat Rev Neurosci. 2006; 7:335–346. [PubMed: 16760914]

Halliday GM, Del Tredici K, Braak H. Critical appraisal of brain pathology staging related to presymptomatic and symptomatic cases of sporadic Parkinson's disease. J Neural Transm Suppl. 2006:99–103. [PubMed: 17017515]

Hantraye P, Varastet M, Peschanski M, Riche D, Cesaro P, Willer JC, Maziere M. Stable parkinsonian syndrome and uneven loss of striatal dopamine fibres following chronic MPTP administration in baboons. Neuroscience. 1993; 53:169–178. [PubMed: 8469305]

Herrero MT, Hirsch EC, Javoy-Agid F, Obeso JA, Agid Y. Differential vulnerability to 1-methyl-4-phenyl-1,2,3,6-tetrahydropyridine of dopaminergic and cholinergic neurons in the monkey mesopontine tegmentum. Brain Res. 1993; 624:281–285. [PubMed: 7902770]

Hilaire G, Viemari JC, Coulon P, Simonneau M, Bevengut M. Modulation of the respiratory rhythm generator by the pontine noradrenergic A5 and A6 groups in rodents. Respir Physiol Neurobiol. 2004; 143:187–197. [PubMed: 15519555]

Jardanhazi-Kurutz D, Kummer MP, Terwel D, Vogel K, Dyrks T, Thiele A, Heneka MT. Induced LC degeneration in APP/PS1 transgenic mice accelerates early cerebral amyloidosis and cognitive deficits. Neurochem Int. 2010; 57:375–382. [PubMed: 20144675]

Jones BE, Moore RY. Ascending projections of the locus coeruleus in the rat. II. Autoradiographic study. Brain Res. 1977; 127:25–53. [PubMed: 301051]

Jones BE, Halaris AE, McIlhany M, Moore RY. Ascending projections of the locus coeruleus in the rat. I. Axonal transport in central noradrenaline neurons. Brain Res. 1977; 127:1–21. [PubMed: 67877]

Kawasaki Y, Kumamoto E, Furue H, Yoshimura M. Alpha 2 adrenoceptor-mediated presynaptic inhibition of primary afferent glutamatergic transmission in rat substantia gelatinosa neurons. Anesthesiology. 2003; 98:682–689. [PubMed: 12606912]

Langston JW, Forno LS, Rebert CS, Irwin I. Selective nigral toxicity after systemic administration of 1-methyl-4-phenyl-1,2,5,6-tetrahydropyrine (MPTP) in the squirrel monkey. Brain Res. 1984; 292:390–394. [PubMed: 6607092]

Lindvall O, Bjorklund A, Nobin A, Stenevi U. The adrenergic innervation of the rat thalamus as revealed by the glyoxylic acid fluorescence method. J Comp Neurol. 1974; 154:317–347. [PubMed: 4826099]

Liprando LA, Miner LH, Blakely RD, Lewis DA, Sesack SR. Ultrastructural interactions between terminals expressing the norepinephrine transporter and dopamine neurons in the rat and monkey ventral tegmental. Synapse. 2004; 52:233–244. [PubMed: 15103690]

Marien M, Briley M, Colpaert F. Noradrenaline depletion exacerbates MPTP-induced striatal dopamine loss in mice. Eur J Pharmacol. 1993; 236:487–489. [PubMed: 7689466]

Marsh L, Biglan K, Gerstenhaber M, Williams JR. Atomoxetine for the treatment of executive dysfunction in Parkinson's disease: a pilot open-label study. Mov Disord. 2009; 24:277–282. [PubMed: 19025777]

Masilamoni G, Votaw J, Howell L, Villalba RM, Goodman M, Voll RJ, Stehouwer J, Wichmann T, Smith Y. (18)F-FECNT: validation as PET dopamine transporter ligand in parkinsonism. Exp Neurol. 2010; 226:265–273. [PubMed: 20832405]

Masilamoni GJ, Bogenpohl JW, Alagille D, Delevich K, Tamagnan G, Votaw JR, Wichmann T, Smith Y. Metabotropic glutamate receptor 5 antagonist protects dopaminergic and noradrenergic neurons from degeneration in MPTP-treated monkeys. Brain. 2011; 134:2057–2073. [PubMed: 21705423]

Mavridis M, Degryse AD, Lategan AJ, Marien MR, Colpaert FC. Effects of locus coeruleus lesions on parkinsonian signs, striatal dopamine and substantia nigra cell loss after 1-methyl-4-phenyl-1,2,3,6-tetrahydropyridine in monkeys: a possible role for the locus coeruleus in the progression of Parkinson's disease. Neuroscience. 1991; 41:507–523. [PubMed: 1870701]

Mejias-Aponte CA, Drouin C, Aston-Jones G. Adrenergic and noradrenergic innervation of the midbrain ventral tegmental area and retrorubral field: prominent inputs from medullary homeostatic centers. J Neurosci. 2009; 29:3613–3626. [PubMed: 19295165]

Mitchell IJ, Cross AJ, Sambrook MA, Crossman AR. Sites of the neurotoxic action of 1-methyl-4-phenyl-1,2,3,6-tetrahydropyridine in the macaque monkey include the ventral tegmental area and the locus coeruleus. Neurosci Lett. 1985; 61:195–200. [PubMed: 3878482]

Mourlevat S, Troadec JD, Ruberg M, Michel PP. Prevention of dopaminergic neuronal death by cyclic AMP in mixed neuronal/glial mesencephalic cultures requires the repression of presumptive astrocytes. Mol Pharmacol. 2003; 64:578–586. [PubMed: 12920193]

Nagatsu I, Kobayashi K, Fujii T, Komori K, Sekiguchi K, Titani K, Fujita K, Nagatsu T. Antibodies raised against different oligopeptide segments of human dopamine-beta-hydroxylase. Neurosci Lett. 1990; 120:141–145. [PubMed: 2293101]

Nieuwenhuys R, Veening JG, van Domburg P. Core and paracores; some new chemoarchitectural entities in the mammalian neuraxis. Acta Morphol Neerl Scand. 1988; 26:131–163. [PubMed: 2908161]

Olanow, C., Stocchi, F., Lang, A. Parkinson's Disease: Non-motor and Non-dopaminergic Features. Wiley-Blackwell; Oxford, UK: 2011. p. 474

Otmakhova NA, Lewey J, Asrican B, Lisman JE. Inhibition of perforant path input to the CA1 region by serotonin and noradrenaline. J Neurophysiol. 2005; 94:1413–1422. [PubMed: 15888529]

Paladini CA, Fiorillo CD, Morikawa H, Williams JT. Amphetamine selectively blocks inhibitory glutamate transmission in dopamine neurons. Nat Neurosci. 2001; 4:275–281. [PubMed: 11224544]

Parent A, Hazrati LN. Functional anatomy of the basal ganglia. II. The place of sub-thalamic nucleus and external pallidum in basal ganglia circuitry. Brain Res Brain Res Rev. 1995; 20:128–154. [PubMed: 7711765]

Peters A, Palay SL, Webster de F. The Fine Structure of the Nervous System: Neurons and Their Supporting Cells. 1991; 2

Phillipson OT. Afferent projections to the ventral tegmental area of Tsai and interfascicular nucleus: a horseradish peroxidase study in the rat. J Comp Neurol. 1979; 187:117–143. [PubMed: 489776]

Pifl C, Schingnitz G, Hornykiewicz O. Effect of 1-methyl-4-phenyl-1,2,3,6-tetrahydropyridine on the regional distribution of brain monoamines in the rhesus monkey. Neuroscience. 1991; 44:591–605. [PubMed: 1754053]

Pintor L, Bailles E, Valldeoriola F, Tolosa E, Marti MJ, de Pablo J. Response to 4-month treatment with reboxetine in Parkinson's disease patients with a major depressive episode. Gen Hosp Psychiatry. 2006; 28:59–64. [PubMed: 16377367]

Remy P, Doder M, Lees A, Turjanski N, Brooks D. Depression in Parkinson's disease: loss of dopamine and noradrenaline innervation in the limbic system. Brain. 2005; 128:1314–1322. [PubMed: 15716302]

Rinaman L. Hindbrain noradrenergic lesions attenuate anorexia and alter central cFos expression in rats after gastric viscerosensory stimulation. J Neurosci. 2003; 23:10084–10092. [PubMed: 14602823]

Rommelfanger KS, Weinshenker D, Miller GW. Reduced MPTP toxicity in noradrenaline transporter knockout mice. J Neurochem. 2004; 91:1116–1124. [PubMed: 15569255]

Schmitz C, Hof PR. Design-based stereology in neuroscience. Neuroscience. 2005; 130:813–831. [PubMed: 15652981]

Simon H, Le Moal M, Stinus L, Calas A. Anatomical relationships between the ventral mesencephalic tegmentum–a 10 region and the locus coeruleus as demonstrated by anterograde and retrograde tracing techniques. J Neural Transm. 1979; 44:77–86. [PubMed: 220380]

Snoddy AM, Tessel RE. Prazosin: effect on psychomotor-stimulant cues and loco-motor activity in mice. Eur J Pharmacol. 1985; 116:221–228. [PubMed: 3878298]

Snyder SH, D'Amato RJ. MPTP: a neurotoxin relevant to the pathophysiology of Parkinson's disease The 1985 George C Cotzias lecture. Neurology. 1986; 36:250–258. [PubMed: 3080696]

Sotiriou E, Vassilatis DK, Vila M, Stefanis L. Selective noradrenergic vulnerability in alpha-synuclein transgenic mice. Neurobiol Aging. 2010; 31:2103–2114. [PubMed: 19152986]

Srinivasan J, Schmidt WJ. Potentiation of parkinsonian symptoms by depletion of locus coeruleus noradrenaline in 6-hydroxydopamine-induced partial degeneration of substantia nigra in rats. Eur J Neurosci. 2003; 17:2586–2592. [PubMed: 12823465]

Srinivasan J, Schmidt WJ. Behavioral and neurochemical effects of noradrenergic depletions with N-(2-chloroethyl)-N-ethyl-2-bromobenzylamine in 6-hydroxydopamine-induced rat model of Parkinson's disease. Behav Brain Res. 2004; 151:191–199. [PubMed: 15084435]

Swanson LW, Hartman BK. The central adrenergic system. An immunofluorescence study of the location of cell bodies and their efferent connections in the rat utilizing dopamine-beta-hydroxylase as a marker. J Comp Neurol. 1975; 163:467–505. [PubMed: 1100685]

Traver S, Salthun-Lassalle B, Marien M, Hirsch EC, Colpaert F, Michel PP. The neurotransmitter noradrenaline rescues septal cholinergic neurons in culture from degeneration caused by low-level oxidative stress. Mol Pharmacol. 2005; 67:1882–1891. [PubMed: 15784847]

Troadec JD, Marien M, Darios F, Hartmann A, Ruberg M, Colpaert F, Michel PP. Noradrenaline provides long-term protection to dopaminergic neurons by reducing oxidative stress. J Neurochem. 2001; 79:200–210. [PubMed: 11595772]

Vogt BA, Hof PR, Friedman DP, Sikes RW, Vogt LJ. Norepinephrinergic afferents and cytology of the macaque monkey midline, mediodorsal, and intralaminar thalamic nuclei. Brain Struct Funct. 2008; 212:465–479. [PubMed: 18317800]

Wikberg JE. Adrenergic receptors: classification, ligand binding and molecular properties. Acta Medica Scand Suppl. 1982; 665:19–36.

Zarow C, Lyness SA, Mortimer JA, Chui HC. Neuronal loss is greater in the locus coeruleus than nucleus basalis and substantia nigra in Alzheimer and Parkinson diseases. Arch Neurol. 2003; 60:337–341. [PubMed: 12633144]

Zweig RM, Cardillo JE, Cohen M, Giere S, Hedreen JC. The locus ceruleus and dementia in Parkinson's disease. Neurology. 1993; 43:986–991. [PubMed: 8492957]
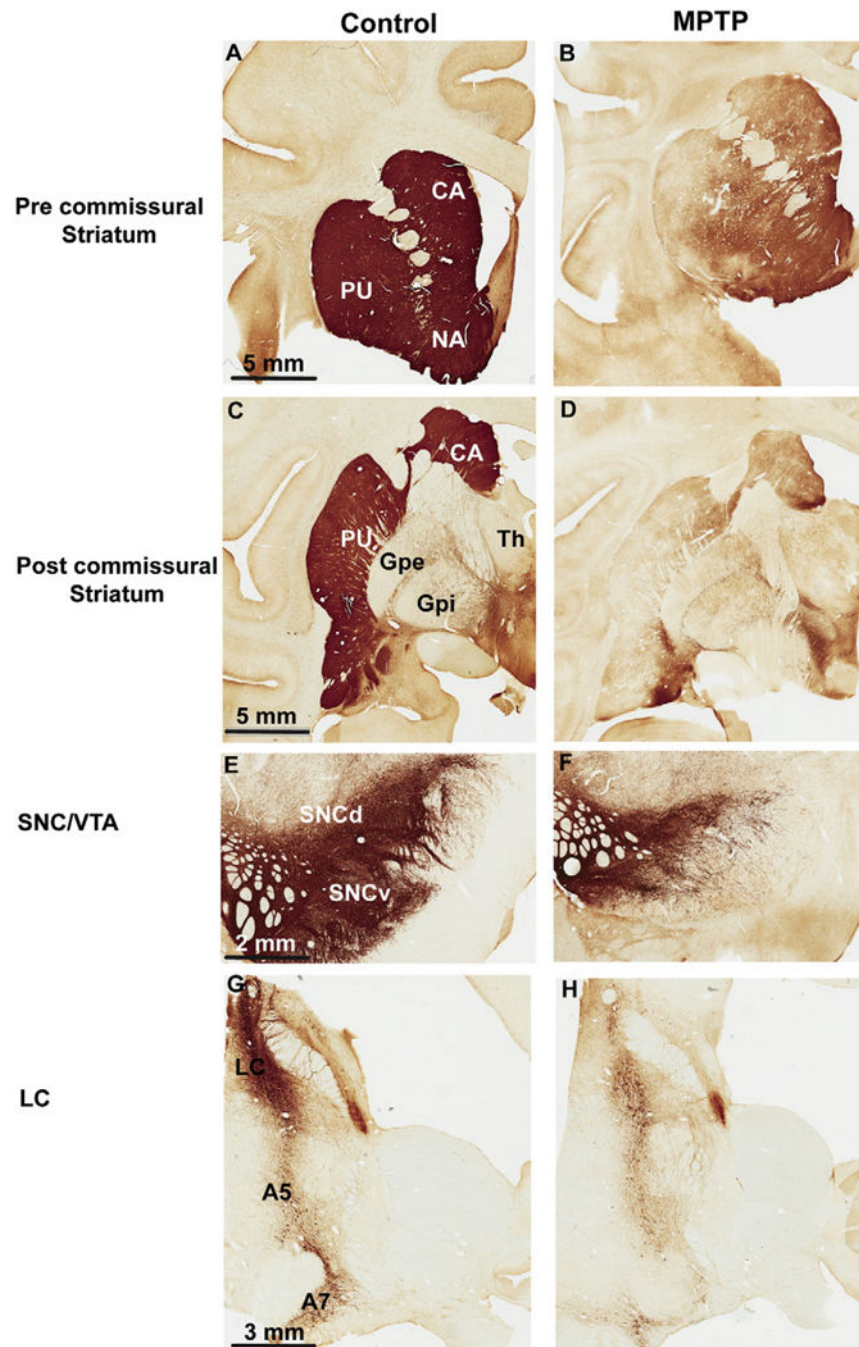
Fig. 1.
Photomicrographs of TH-immunostained coronal sections at the level of the pre-commissural striatum (A–B), post-commissural striatum (C–D), midbrain dopaminergic cell groups (E–F) and noradrenergic cells groups (G, H) of a control (left column) and a MPTP-treated (right column) monkey. Abbreviations: A5, A7: Noradrenergic cell groups A5 and A7; CA: caudate nucleus; GPe: globus pallidus, external segment; GPi: globus pallidus, internal segment; LC: locus coeruleus; PU: putamen; SNCd: substantia nigra compacta,

dorsal tier; SNCv: substantia nigra, ventral tier; Th: thalamus; VTA: ventral tegmental area. Scale bars: A–D = 5 mm, E–F = 2 mm, G–H = 2 mm.
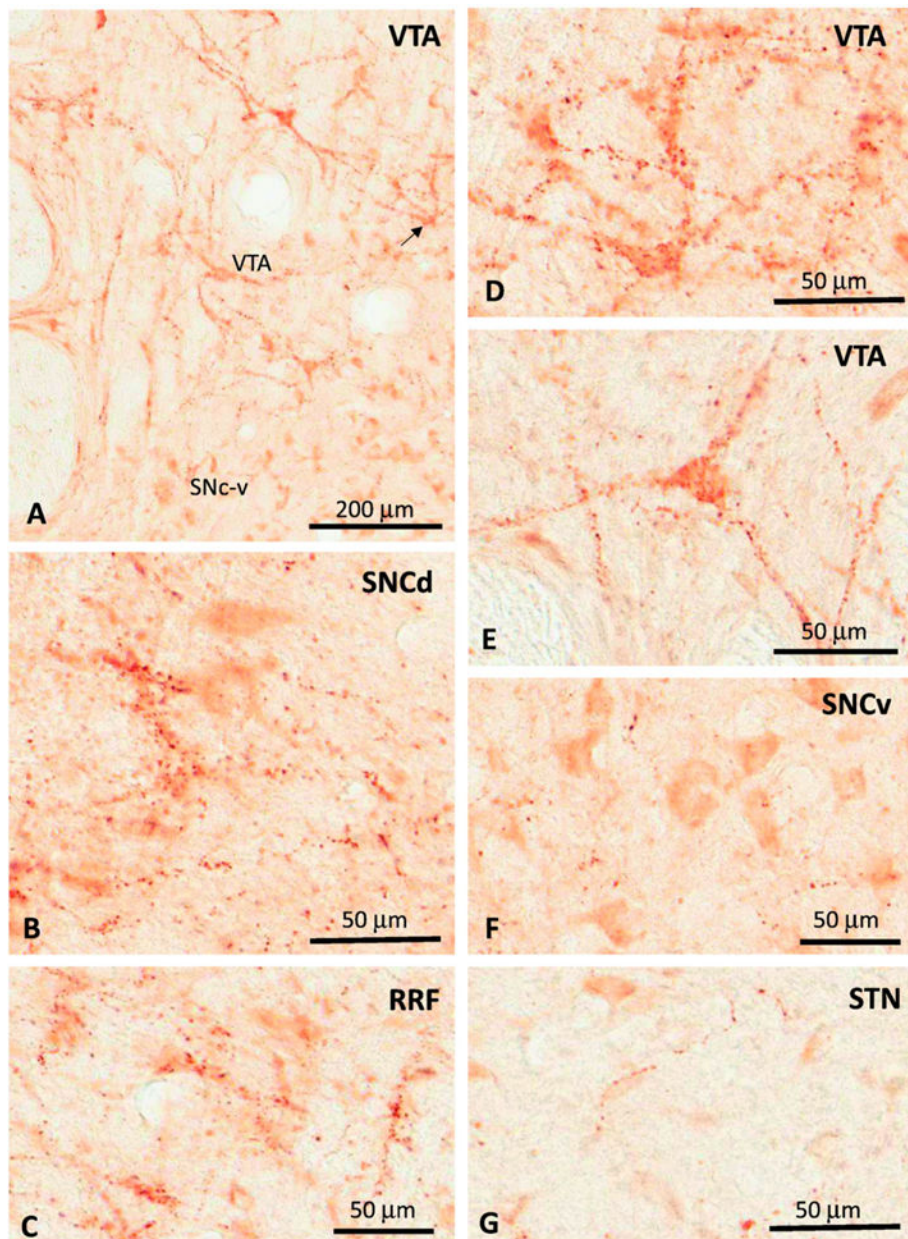
Fig. 2.
Photomicrographs of DβH-immunoreactive axonal profiles and terminal-like varicosities in the VTA (A, D, E), SNc-d (B), RRF (C), SNc-v (F) and STN (G) of a normal rhesus monkey. See text for abbreviations. Scale bars: A = 200 μm B–G = 50 μm.
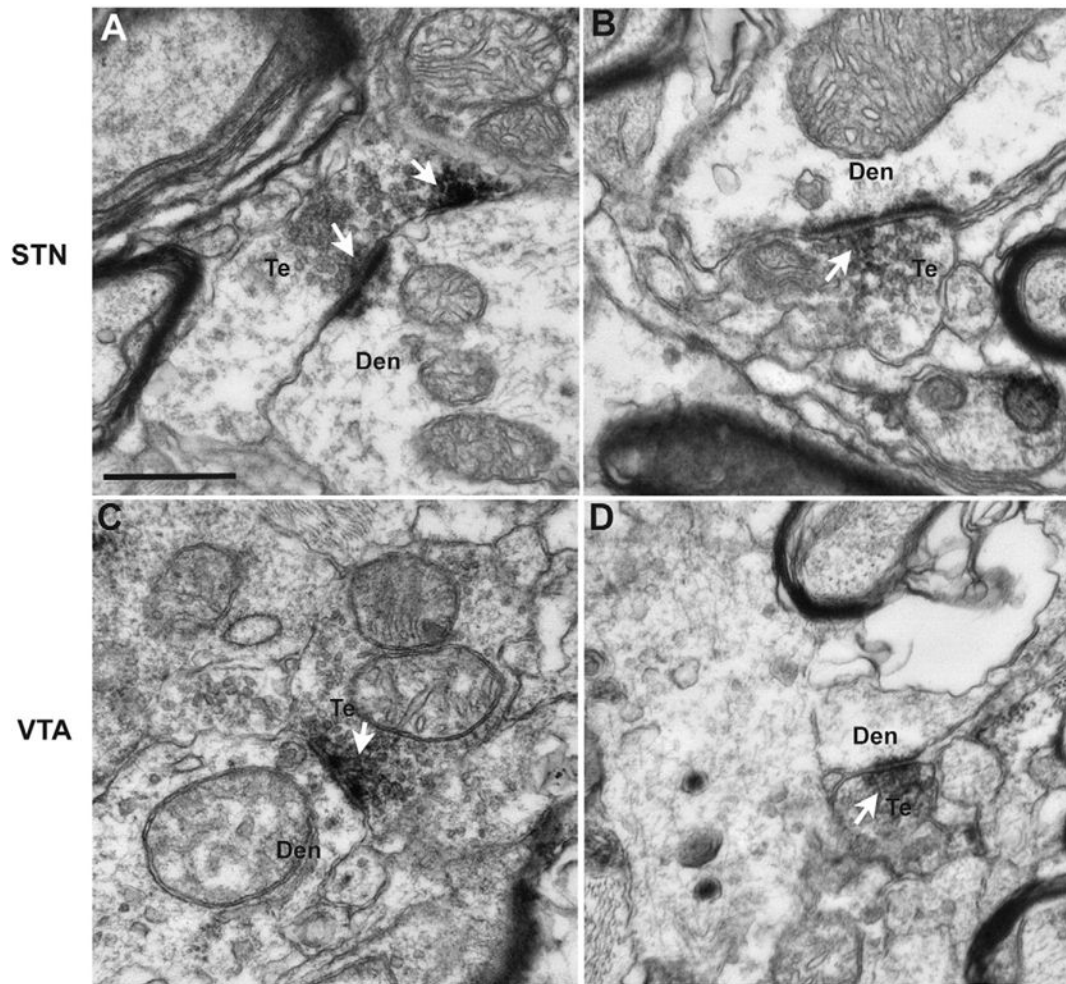
Fig. 3.
Electron micrographs of DβH-positive terminals (Te) that form asymmetric axo-dendritic synapses in the STN (A, B) and VTA (C, D) of a normal rhesus monkey. The arrows indicate aggregates of peroxidase deposit confined to pre-synaptic vesicles in the active zones of asymmetric axo-dendritic synapses formed by these terminals. Abbreviation: Den (dendrite). Scale bars: A–D = 500 nm.
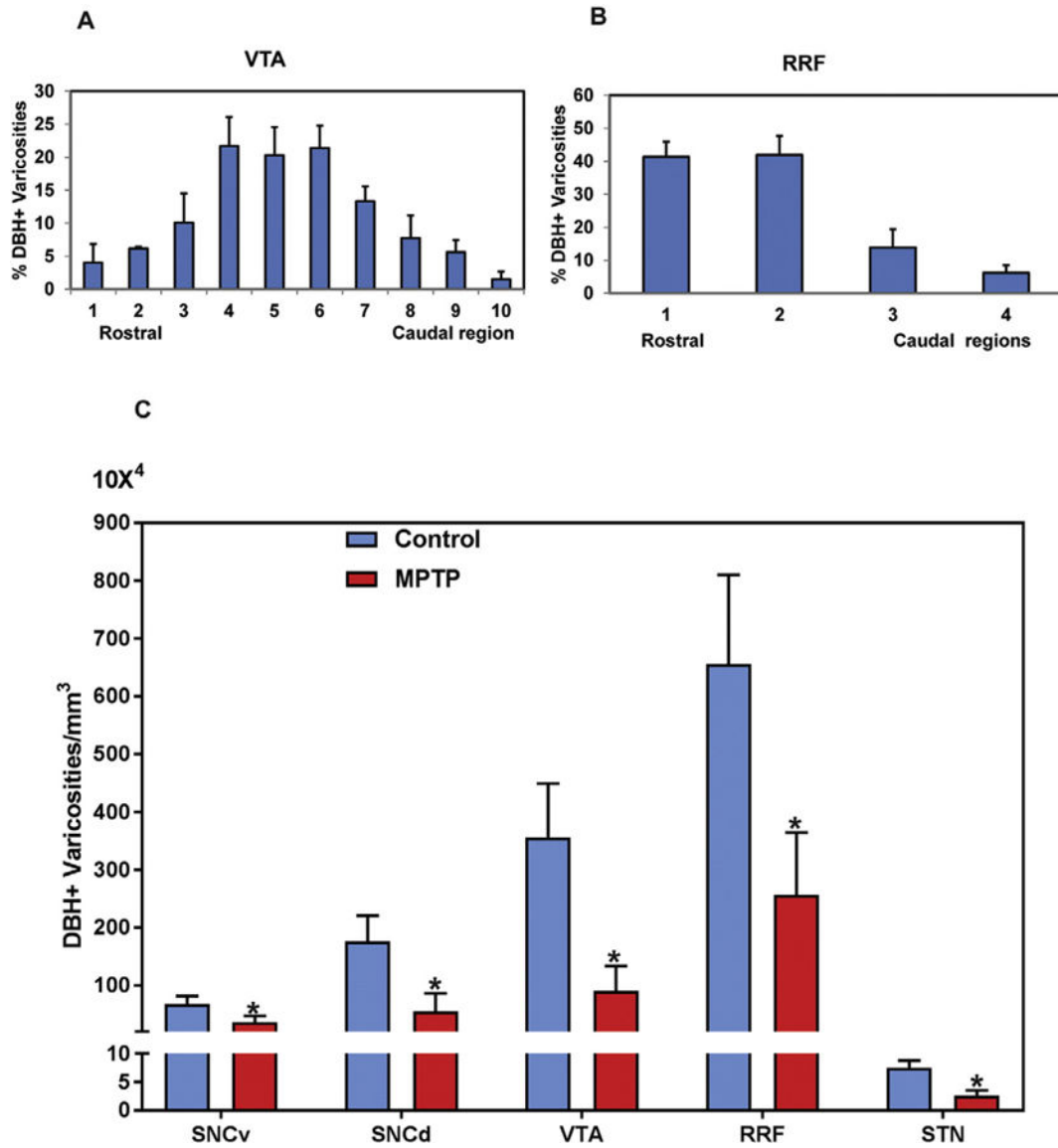
Fig. 4.
(A, B) Relative percentages of DβH-positive varicosities along the rostrocaudal extent of the VTA and RRF in normal monkeys. (C) Comparison of the estimated density of DβH-positive varicosities (means ± SD) in the various ventral midbrain dopaminergic cells groups (SNCv, SNCd, VTA, RRF) and the STN between control and MPTP-treated parkinsonian monkeys.* $P < 0.001$ for differences between control, and MPTP-treated animals by using one-way ANOVA with Tukey's post hoc test.
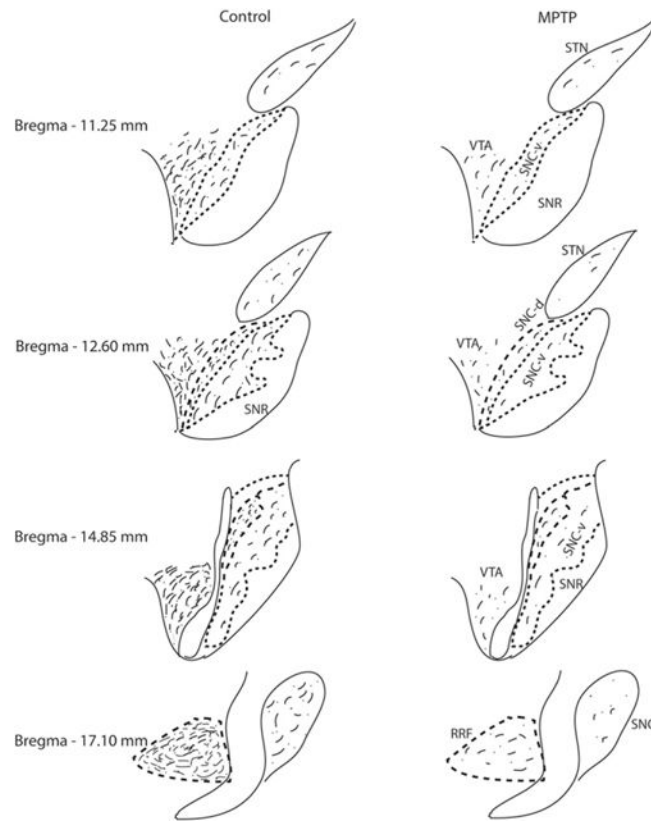
Fig. 5.
Schematic diagram to illustrate the relative density and distribution of DβH-containing axonal profiles through the ventral midbrain dopaminergic cell groups (SNCv, SNCv, SNCd, VTA, RRF) and the STN of controls and MPTP-treated monkeys. The SN pars reticulate (SNr) was almost completely devoid of DβH-immunoreactive profiles.

Table 1

Primary antibodies used in this study.

Antibody	Immunogen	Manufacturer data	Dilution
Tyrosine Hydroxylase	Tyrosine Hydroxylase purified from PC12 cells	Millipore (MAB 318), Mouse monoclonal	1:1000
Calbindin-D-28K	Bovine kidney calbindin-D	Sigma (C-9848) Mouse monoclonal	1: 4000
Dopamine-beta-hydroxylase	Synthetic peptide, CPTSQGRSPAGPTVVSI-amide, cloned from human (DbH) cDNA (Nagatsu et al., 1990)	Millipore (AB 1536), Rabbit polyclonal	1:500